

1 E-mail: yjhong@chonnam.ac.kr

2

3 **Short running title:** Targeting calreticulin for imaging immunogenic cell death

4

5 **Total word count of the manuscript:** 3078

6

7 **Financial support:** This study was supported by a grants from the National Research Foundation (NRF)
8 of Korea (NRF-2017R1A2B3012157 and NRF-2018M3A9H3024850) and the
9 Pioneer Research Center Program (2015M3C1A3056410), funded by the Ministry
10 of Science and ICT (MSIT). D.-Y.K. was supported by the NRF grant funded by
11 MSIT (NRF-2020R1C1C1012379) and A.P. was supported by the Basic Science
12 Research Program through the NRF of Korea funded by the Ministry of Education
13 (NRF-2020R1I1A1A01070543). Y.H. was supported by an NRF of Korea grant,
14 funded by the Korean government (MSIT; No.2018R1A5A2024181).

15

16 **Disclosure:** The authors have no competing interests to declare.

17

18

1 **ABSTRACT**

2 Surface-exposed calreticulin (ecto-CRT) is a well-known ‘eat-me’ signal exhibited by dying
3 cells that contributes to their recognition and destruction by the immune system. We assessed the use of a
4 CRT-specific binding peptide for imaging ecto-CRT during immunogenic cell death and its utility for the
5 early prediction of treatment response. **Methods:** A synthetic CRT-specific peptide KLGFFKR (CRTpep)
6 was labeled with fluorescein isothiocyanate or ¹⁸F and characteristics of ecto-CRT was evaluated in colon
7 cancer cell line *in vitro* and *in vivo*. **Results:** *In vitro* flow cytometry, immunofluorescence staining, and
8 *in vivo* micro positron emission tomography imaging results showed that CRTpep detected pre-apoptotic
9 cells treated with immunogenic drugs or radiation, but not those treated with the non-immunogenic drug
10 or a non-therapeutic dose of immunogenic drug. **Conclusion:** The present results indicate that the CRT-
11 specific peptide would enable the prediction of therapeutic response, thereby facilitating early decisions
12 regarding the continuation or discontinuation of immunogenic treatment.

13

14

1 INTRODUCTION

2 Calreticulin (CRT), a Ca^{2+} binding protein mainly located in the lumen of the endoplasmic
3 reticulum (1). Surface exposure of CRT (ecto-CRT) can be induced by certain chemotherapeutic agents
4 (e.g., oxaliplatin (OXP), mitoxantrone (MTX), and doxorubicin (DXR)) and ionizing radiation, and
5 occurs within 1–4 h from the induction of immunogenic cell death (ICD), before the cells become
6 apoptotic (2-7). By contrast, lethal stimuli that fail to elicit sufficient ER stress, such as the non-
7 immunogenic drugs gemcitabine (GEM), mitomycin C, and cisplatin, do not induce the immunogenic
8 exposure of CRT on the cell surface unless an exogenous source of ER stress is provided (8,9).

9 In cancer therapy, the ability to predict the response to treatment as early as possible is highly
10 desirable. However, modern medical imagings such as computed tomography and positron emission
11 tomography (PET) require several weeks to months to predict responsiveness. Thus, molecular imaging
12 technologies that can characterize and measure biological processes at the cellular and molecular level in
13 living subjects (10,11) are eagerly anticipated.

14 The KLGFFKR peptide motif in the cytoplasmic domain of an integrin that interacts with CRT to
15 induce Ca^{2+} binding has potential as an imaging probe for targeting ecto-CRT (12). We labeled the
16 KLGFFKR peptide sequence (CRTpep) with fluorescein isothiocyanate (FITC) or ^{18}F , and evaluated its
17 ability to detect dying cancer cells *in vitro* and *in vivo* after treatment with chemotherapeutic drugs or
18 radiation.

1 MATERIALS AND METHODS

2 Radiochemistry for ¹⁸F-CRTpep synthesis

3 Calreticulin peptide (CRTpep), CRTpep-FITC (KLGFFKR and KLGFFKR-FITC) and ¹⁹F-
4 CRTpep (reference compound) were synthesized by Anygen Co., South Korea (Supplemental Fig. 1-3).
5 *N*-succinimidyl 4-fluorobenzoate (SFB) and ethyl 4-(trimethyl-ammonium) benzoate (¹⁸F-SFB precursor)
6 were prepared as previously described (13,14), with some modifications. ¹⁸F-CRTpep was synthesized
7 using modifications of previously reported methods (15,16). First, ¹⁸F-SFB was synthesized to an
8 approximately 30–40% (non-decay corrected) radiochemical yield; the radiochemical purity was > 98%.
9 A fraction of the ¹⁸F-SFB solution in HPLC eluent was added to a reaction vessel and evaporated.
10 CRTpep solution (2.0 mg, 2.235 μmol) in borate buffer (pH 8.5, 0.1 M) was added to evaporated ¹⁸F-SFB
11 and incubated for 30 min at 40°C. Finally, the crude ¹⁸F-CRTpep (¹⁸F-SFB conjugated CRTpep) was
12 cooled and injected into a semi-preparative HPLC column system for purification (with the same gradient
13 as used for the isolation of the reference compound). For identification of the ¹⁸F-CRTpep, the collected
14 HPLC fraction (purified ¹⁸F-SFB) was co-injected with the ¹⁹F-CRTpep. The radiochemical yield of ¹⁸F-
15 CRTpep was approximately 15–20% (non-decay corrected) and the radiochemical purity was > 98%
16 according to the analytical HPLC system. ¹⁸F-CRTpep was dried, made isotonic with sodium chloride,
17 and passed through a 0.2 micron membrane.

18

19 *In vivo* Mouse Models and Small Animal PET Studies

20 The antitumor activity of the chemotherapy and radiation was evaluated in CT26 (murine
21 colorectal carcinoma)-bearing BALB/c mice and B16F10 (murine melanoma)-bearing C57BL/6 mice
22 when tumors reached approximately 100 mm³ after implantation. Mice were injected intravenously with
23 doxorubicin (5 mg/kg or 10 mg/kg), and intraperitoneally with oxaliplatin (5 mg/kg) and gemcitabine (15
24 mg/kg) three times with a 2 day interval between each dose. Radiation therapy (15 Gy) was given once

1 using a linear accelerator (CLINAC 21EX, Varian, Palo Alto, USA) emitting 10 MV X-rays to deliver a
2 dose rate of 3 Gy/min at a source to skin distance of 100 mm and a field size of $5 \times 5 \text{ cm}^2$ (17). Small
3 animal PET studies were performed immediately before and after treatment; 6 days after the start of (2
4 days after the last dose of) oxaliplatin (5 mg/kg, n = 3), doxorubicin (5 or 10 mg/kg, n = 3, each),
5 gemcitabine (15 mg/kg, n = 3), or radiation therapy (15 Gy, n = 3). Images were acquired 1 and 2 h after
6 intravenous injection of 2-deoxy-2-¹⁸F-fluoro-D-glucose (¹⁸F-FDG; 7.4 MBq/200 μ L) and ¹⁸F-CRTpep
7 (7.4 MBq/200 μ L), respectively. Both studies were performed on the same animal at 8 h intervals. All
8 animal studies were conducted in accordance with the principles and procedures outlined in the National
9 Institutes of Health (NIH) Guide for the Care and Use of Animals (18) and using protocols approved by
10 the Animal Care and Use Committee of Chonnam National University.

11

1 RESULTS

2 Pre-apoptotic Cell Death and Surface Exposure of CRT after Treatment

3 Oxaliplatin at 500 μ M, doxorubicin at 25 μ M, mitoxantrone at 3 μ M, and gemcitabine at 15 μ M
4 were the doses chosen for analysis of pre-apoptotic markers and ecto-CRT based on apoptotic cell death
5 rates < 20% at 2 and 4 h after drug exposure (Supplemental Fig. 4, and 5). The expression of ER stress
6 and pre-apoptotic markers (pEIF2 α , pPERK, and Cas-8) was significantly higher (2 and 4 h) in oxaliplatin,
7 doxorubici, mitoxantron, and gemcitabine -treated cells than in untreated cells (Fig. 1A, and 1B),
8 demonstrating the early phase of apoptosis in response to the treatments with selected doses. Treatment
9 with oxaliplatin, doxorubici, mitoxantrone, and radiation (2, 5, and 10 Gy) significantly increased ecto-
10 CRT in CT26 cells, whereas the non-immunogenic drug gemcitabine had no effect (Fig. 1C;
11 Supplemental Fig. 6). In addition, doxorubicin treatment significantly increased the expression of ecto-
12 CRT in CT26 xenografts (Supplemental Fig. 7). This demonstrated that CRT translocation was
13 specifically induced by immunogenic drugs and radiation in pre-apoptotic CT26 cells.

14

15 Specific Binding of CRTpep to Ecto-CRT

16 The CRTpep was shown to have a micromolar affinity ($K_d = 1.868 \mu$ M; Supplemental Fig. 8).
17 Specific binding of CRTpep to ecto-CRT was examined in CT26 and B16F10 cells before and treatment.
18 Flow cytometry analysis and confocal fluorescence microscopy showed that CRTpep detected oxaliplatin,
19 doxorubicin, and mitoxantrone-treated pre-apoptotic cells. By contrast, no significant binding was
20 observed in gemcitabine-treated cells or in untreated cells (Fig. 2, and 3; Supplemental Fig. 9, and 10).
21 Cell surface binding of FITC-CRTpep was decreased significantly by pre-treatment with 200 μ M of
22 unlabeled CRTpep, indicating that the fluorescence detected corresponded to bound ecto-CRT (Fig. 2,
23 and 3; Supplemental Fig. 9, and 10). Overall, these results indicate that CRTpep targets ecto-CRT
24 specifically in cells undergoing early ICD.

25

1 ¹⁸F-CRTpep Small Animal PET Imaging of Immunogenic Cancer Cell Death

2 Subsequently, we employed ¹⁸F-CRTpep for *in vitro* and *in vivo* studies. ¹⁸F-CRTpep showed
3 high stability for 2 h (over 90%) (Supplemental Fig. 11). Cellular uptake of ¹⁸F-CRTpep significantly
4 increased after DXR treatment (Supplemental Fig. 12). Next, we examined the potential of CRTpep for
5 the detection of ICD induction *in vivo* with the ultimate aim of imaging tumor responses to immunogenic
6 chemotherapy and radiotherapy. First, we assessed the tumor reductive effect of chemotherapeutic agents
7 and radiotherapy. Doxorubicin, oxaliplatin, gemcitabine, or radiotherapy significantly suppressed tumor
8 growth in CT26-bearing BALB/c mice (responder), whereas treatment with a non-therapeutic dose of
9 doxorubicin (5 mg/kg) or phosphate buffered saline (PBS) had no effect (non-responder). Tumor volume
10 between responder and non-responder was not significantly different until 6 days after treatment, but
11 became significantly different thereafter (Supplemental Fig. 13). Small animal PET imaging showed a
12 significant ¹⁸F-CRTpep signal in CT26 and B16F10 xenografts 6 days post-treatment with therapeutic
13 dose of doxorubicin, oxaliplatin, or radiation (Fig. 4A and 4B; Supplemental Video, Supplemental Fig.
14 14). No significant signal was detected in the tumors of mice before treatment, or in those treated with
15 gemcitabin, non-therapeutic dose of doxorubicin or PBS. ¹⁸F-CRTpep uptake in 10 mg/kg doxorubicin -
16 treated tumors was 29.7 ± 2.8 -fold higher than that in tumors of PBS-treated mice at post-treatment days
17 6 (Fig. 4B). PET imaging corresponded with biodistribution study in doxorubicin-treated CT26 xenograft
18 mice (Supplemental Table 1). ¹⁸F-FDG PET, which is widely employed in the clinic, showed no
19 significant difference in tumor uptake between the different treatments (Fig. 4C, and 4D). Taken together,
20 these results indicate that targeting ecto-CRT enables the early measurement of treatment response in the
21 context of ICD.

1 **DISCUSSION**

2 A strong ecto-CRT signal was observed in responsive tumors as early as 6 days after the start of
3 immunogenic treatment, whereas no significant signal was detected in unresponsive tumors or tumors
4 treated with non-immunogenic agents. The tumor uptake of ¹⁸F-CRTpep was observed before the gross
5 tumor suppression was observed and increased 30-fold in doxorubicin-treated tumors compared with
6 untreated tumors. This uptake is considerably higher than that reported previously (19) for a molecular
7 probe targeting surface-exposed histone H1 (ApoPep-1), which showed a 1.6-fold increase in
8 doxorubicin-treated tumors compared with untreated tumors. Accordingly, pre-apoptotic surface-exposed
9 CRT would be more beneficial as a biomarker for determining the fate of cells after cancer treatment.

10 The present study, while lacking data related to the appraisal of an imaging agent (such as
11 binding affinity measurement, pharmacokinetics, and biodistribution), provides proof of principle. Further
12 studies using chemically modified CRTpep and engineered protein scaffolds with high binding affinity
13 and *in vivo* stability are currently underway.

1 **CONCLUSION**

2 Imaging ecto-CRT may be an effective means of identifying tumor cells undergoing apoptosis in
3 response to immunogenic therapy. The ability to recognize a pre-apoptotic state using PET at an early
4 stage of immunogenic treatment has major implications for the early prediction of treatment response,
5 which could improve the clinical outcomes of cancer therapy.

6

1 **ACKNOWLEDGEMENTS**

2 We thank Hwa Youn Jang (Innovation Center for Molecular Probe Development in Chonnam
3 National University Hwasun Hospital) for their excellent research assistance

1 **KEY POINTS**

2 **QUESTION:** Does targeting ecto-CRT visualize of pre-apoptotic cells and eventually enable
3 the early measurement of treatment response in the context of immunogenic cell death?

4
5 **PERTINENT FINDINGS:** Imaging ecto-CRT was an effective means of identifying tumor
6 cells undergoing apoptosis in response to immunogenic therapy. A strong tumor uptake of [¹⁸F]CRTpep
7 was observed before the gross tumor suppression was observed and increased 30-fold in doxorubicin-
8 treated tumors compared with untreated tumors.

9
10 **IMPLICATIONS FOR PATIENT CARE:** The present results offer a new PET technology
11 that would enable the prediction of therapeutic response, thereby facilitating early decisions regarding the
12 continuation or discontinuation of immunogenic treatment

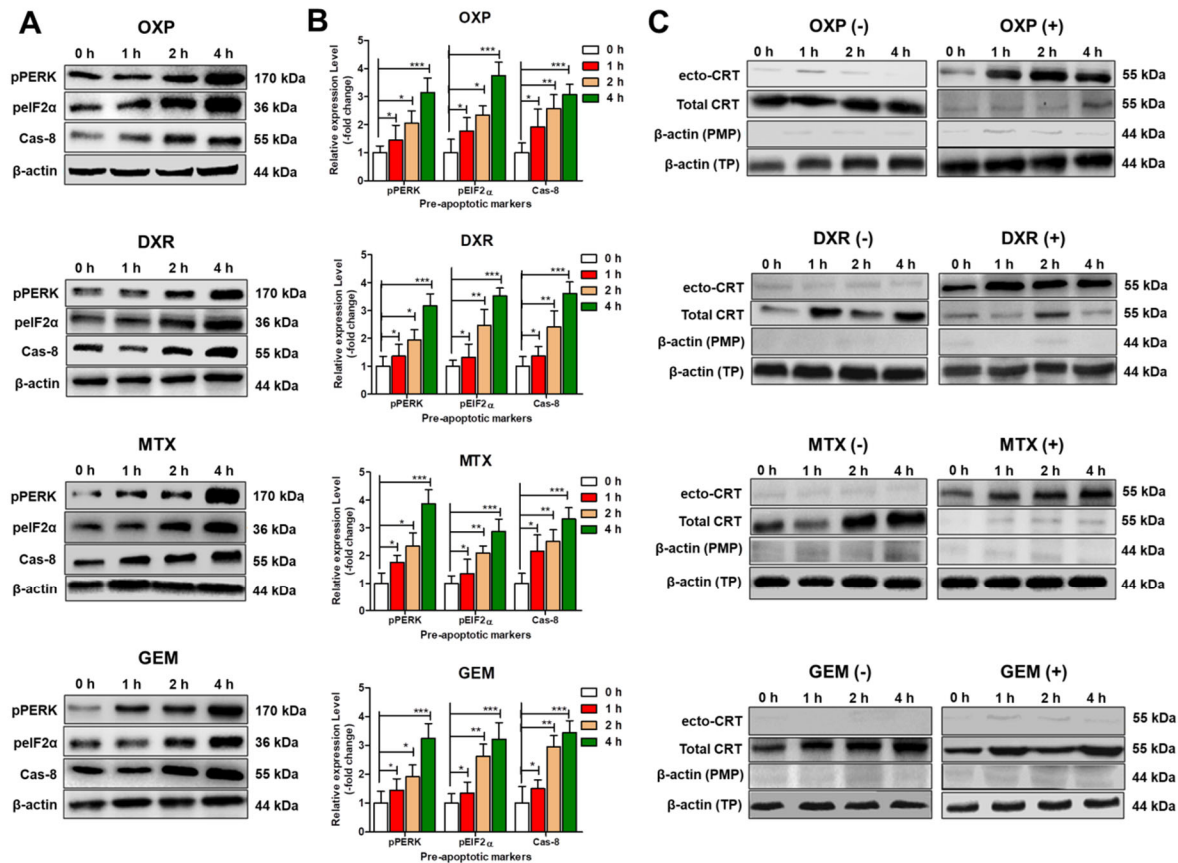
13

1 REFERENCES

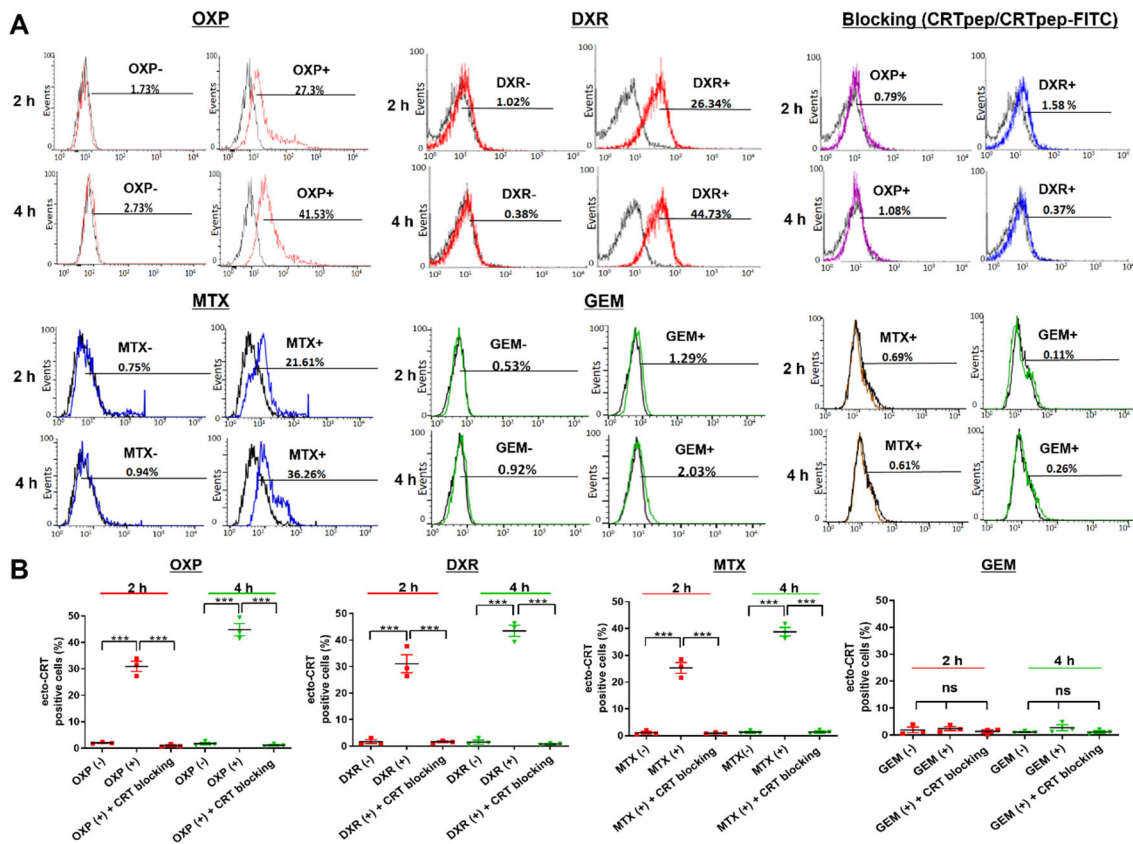
- 2 1. Johnson S, Michalak M, Opas M, Eggleton P. The ins and outs of calreticulin: from the ER
3 lumen to the extracellular space. *Trends Cell Biol.* 2001;11:122-129.
- 4 2. Garg AD, Nowis D, Golab J, Vandenabeele P, Krysko DV, Agostinis P. Immunogenic cell
5 death, DAMPs and anticancer therapeutics: an emerging amalgamation. *Biochim Biophys*
6 *Acta.* 2010;1805:53-71.
- 7 3. Panaretakis T, Kepp O, Brockmeier U, et al. Mechanisms of pre-apoptotic calreticulin
8 exposure in immunogenic cell death. *EMBO J.* 2009;28:578-590.
- 9 4. Green DR, Ferguson T, Zitvogel L, Kroemer G. Immunogenic and tolerogenic cell death.
10 *Nat Rev Immunol.* 2009;9:353-363.
- 11 5. Zitvogel L, Apetoh L, Ghiringhelli F, Kroemer G. Immunological aspects of cancer
12 chemotherapy. *Nat Rev Immunol.* 2008;8:59-73.
- 13 6. Obeid M. ERP57 membrane translocation dictates the immunogenicity of tumor cell death
14 by controlling the membrane translocation of calreticulin. *J Immunol.* 2008;181:2533-2543.
- 15 7. Obeid M, Tesniere A, Ghiringhelli F, et al. Calreticulin exposure dictates the
16 immunogenicity of cancer cell death. *Nat Med.* 2007;13:54-61.
- 17 8. Garg AD, Krysko DV, Verfaillie T, et al. A novel pathway combining calreticulin exposure
18 and ATP secretion in immunogenic cancer cell death. *EMBO J* 2012;31:1062-1079.
- 19 9. Menger L, Vacchelli E, Adjemian S, et al. Cardiac glycosides exert anticancer effects by
20 inducing immunogenic cell death. *Sci Transl Med.* 2012;4:143-199.
- 21 10. Brindle K. New approaches for imaging tumour responses to treatment. *Nat Rev Cancer.*
22 2008;8:94-107.
- 23 11. Willmann JK, Van Bruggen N, Dinkelborg LM, Gambhir SS. Molecular imaging in drug
24 development. *Nat Rev Drug Discov.* 2008;7:591.

- 1 **12.** Kwon MS, Park CS, Choi K, et al. Calreticulin couples calcium release and calcium influx in
2 integrin-mediated calcium signaling. *Mol Biol Cell*. 2000;11:1433-1443.
- 3 **13.** Dissoki S, Hagooly A, Elmachily S, Mishani E. Labeling approaches for the GE11 peptide,
4 an epidermal growth factor receptor biomarker. *J Label Compd Radiopharm*. 2011;54:693-
5 701.
- 6 **14.** Di Gialleonardo V, Signore A, Glaudemans AW, Dierckx RA, De Vries EF. *N*-(4-¹⁸F-
7 fluorobenzoyl)interleukin-2 for PET of human-activated T lymphocytes. *J Nucl Med*.
8 2012;53:679-686.
- 9 **15.** Wang MW, Wang F, Zheng YJ, et al. An in vivo molecular imaging probe ¹⁸F-Annexin B1
10 for apoptosis detection by PET/CT: preparation and preliminary evaluation. *Apoptosis*.
11 2013;18:238-247.
- 12 **16.** Tang G, Tang X, Wang X. A facile automated synthesis of *N*-succinimidyl 4-
13 [¹⁸F]fluorobenzoate ([¹⁸F]SFB) for ¹⁸F-labeled cell-penetrating peptide as PET tracer. *J*
14 *Labelled Comp Radiopharm*. 2010;53:543-547.
- 15 **17.** Jiang SN, Phan TX, Nam TK, et al. Inhibition of tumor growth and metastasis by a
16 combination of Escherichia coli-mediated cytolytic therapy and radiotherapy. *Mol Ther*.
17 2010;18:635-642.
- 18 **18.** NR C. Guide for the care and use of laboratory animals: National Academies Press; . 2010.
- 19 **19.** Wang K, Purushotham S, Lee JY, et al. In vivo imaging of tumor apoptosis using histone
20 H1-targeting peptide. *J Control Release*. 2010;148:283-291.
- 21

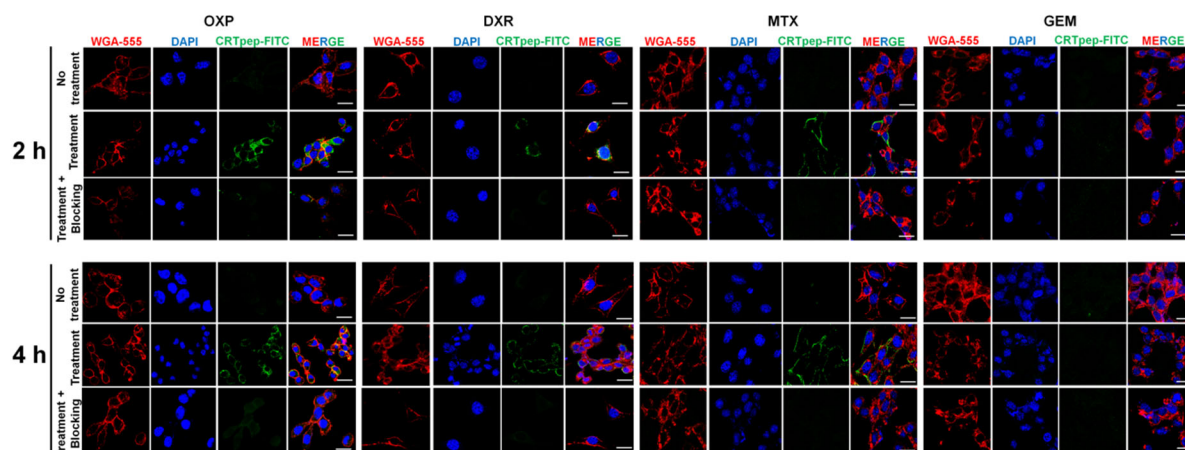
1 **FIGURE WITH LEGENDS**



2
3 **Figure 1. Expression of pre-apoptotic markers and CRT in CT26 cells after immunogenic**
4 **treatment.** CT26 cells were treated with oxaliplatin (OXP, 500 μ M), doxorubicin (DXR, 25 μ M),
5 mitoxantrone (MTX, 3 μ M), or gemcitabine (GEM, 15 μ M) for 0, 1, 2, and 4 h. (A) The levels of pre-
6 apoptotic proteins pPERK, pEIF2 α and Cas-8 were analyzed by western blotting. (B) Expression of pre-
7 apoptotic-related markers pPERK, pEIF2 α and Cas-8 in CT26 cells was quantified using densitometry
8 analysis of western blots after treatment for 0, 1, 2 and 4 h with OXP, DXR, MTX, or GEM. The relative
9 expression was calculated to the respective control using Student's *t*-test, and the level of expression was
10 expressed as the mean of three independent experiments (**P* < 0.05; ***P* < 0.01; ****P* < 0.001; NS = not
11 significant) n = 3. (C) Western blot analysis of translocated CRT (ecto-CRT) in the plasma membrane
12 and total CRT in CT26 cell lysates with and without immunogenic treatment. CT26 cells were treated
13 with or without immunogenic (OXP, DXR, or MTX) and non-immunogenic (GEM) drugs for 0, 1, 2 or 4
14 h.

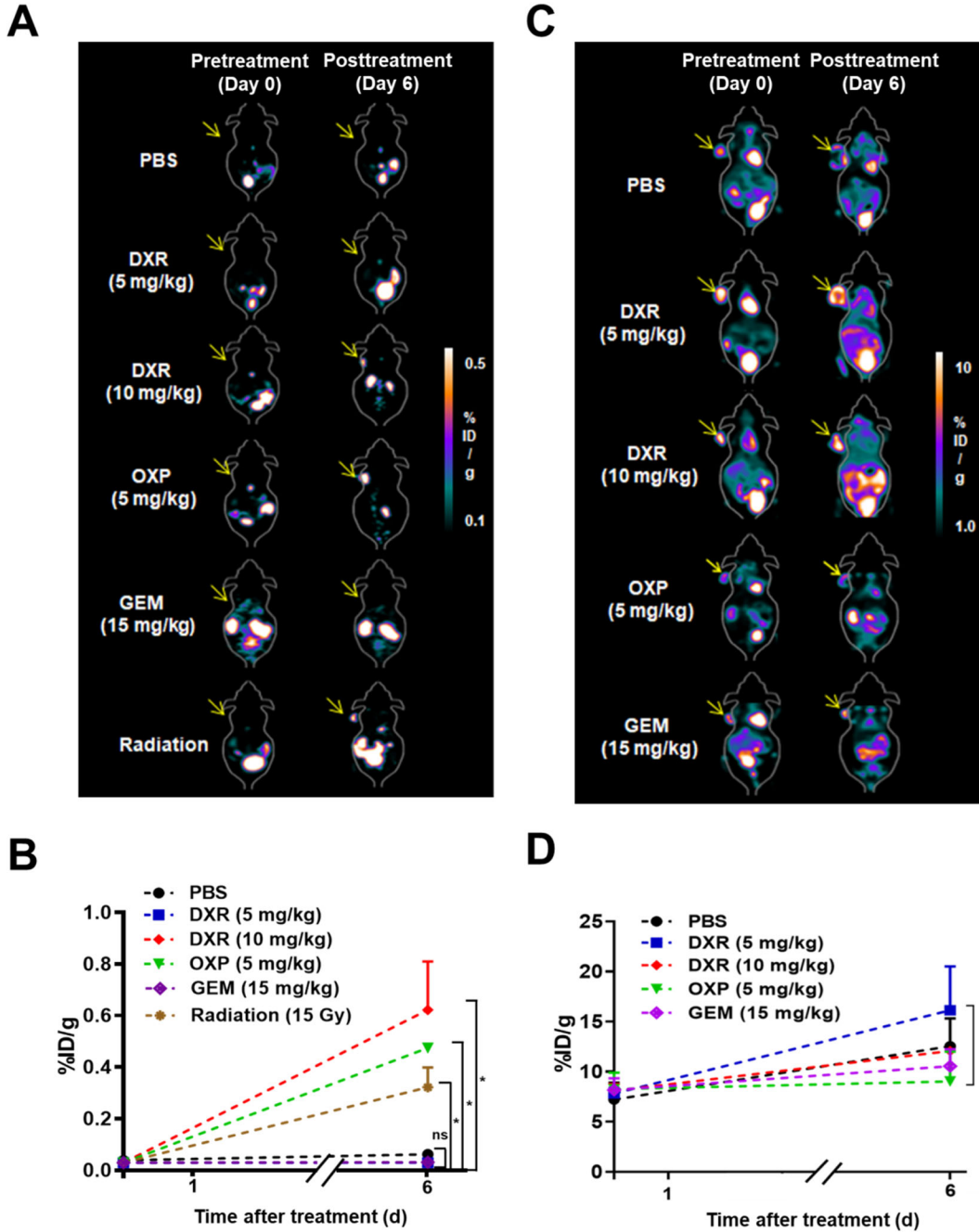


1
2 **Figure 2. Flow cytometry analysis of CRTpep binding to ecto-CRT after immunogenic and non-**
3 **immunogenic drug treatment in CT26 cells. (A)** Flow cytometry analysis of CRTpep binding to ecto-
4 CRT after immunogenic and non-immunogenic drug treatment in CT26 cells. Binding of FITC-CRTpep
5 to ecto-CRT in CT26 cells after 2 h and 4 h of anticancer drug (immunogenic and non-immunogenic)
6 treatment was determined by flow cytometry. Percentage cellular uptake was calculated based on the
7 detected mean fluorescence levels of untreated control cell. After anticancer drug treatment CT26 cells
8 were pre-incubated with CRTpep (200 μ M) for 1 h, followed by incubation with FITC-CRTpep (2 μ M),
9 and then was subjected to flow cytometry to detect uptake using fluorescence generated by the ecto-CRT.
10 **(B)** Quantitative assessment of binding of FITC-CRTpep to ecto-CRT in CT26 cells after 2 h and 4 h of
11 anticancer drug (immunogenic and non-immunogenic) treatment that was determined by flow cytometry.
12 The data were expressed as mean (\pm SD) fluorescence level. (n = 3; *** P < 0.001; NS = not significant).
13



1
 2 **Figure 3. Immunofluorescence staining and analysis of CRTpep binding to ecto-CRT after**
 3 **immunogenic and non-immunogenic drug treatment in CT26 cells.** Binding of FITC-CRTpep to ecto-
 4 CRT in CT26 cells after 2 h and 4 h of anticancer drug (immunogenic and non-immunogenic) treatment
 5 was determined by confocal laser scanning microscopy (40 × magnification) after immunofluorescence
 6 staining. Green, FITC-CRTpep; blue, DAPI-stained nuclei; red, cell membrane stained with WGA-555.
 7 Scale bar, 50 μm. For the blocking assay, anticancer drug-treated cells were further incubated with 200
 8 μM unlabeled CRTpep followed by 2 μM FITC-CRTpep. Scale bar, 50 μm.

9



1
2 **Figure 4. Assessment of ICD by PET using ^{18}F -CRTpep and ^{18}F -FDG in CT26 tumor-bearing mice.**
3 **(A)** Representative ^{18}F -CRTpep PET images of CT26-bearing mice. ^{18}F -CRTpep (7.4 MBq) was injected
4 (*i.v.*) into mice before and at 6 days after chemotherapy or radiotherapy ($n = 4$ per group). Arrows
5 indicate subcutaneous tumors. **(B)** Quantification of ^{18}F -CRTpep PET imaging signals in tumors before
6 (day 0) and after treatment ($*P < 0.05$; NS = not significant; P value of PBS vs doxorubicin (5 mg/kg) or

1 gemcitabine on day 6: = 0.4991 or = 0.9925, respectively). **(C)** Representative ^{18}F -FDG PET images of
2 CT26-bearing mice. ^{18}F -FDG was injected (*i.v.*) into the same mice used at 8 h after the ^{18}F -CRTpep
3 experiments (n = 4 per group). **(D)** Quantification of ^{18}F -FDG PET signals in tumors before (day 0) and
4 after treatment (NS = not significant)
5

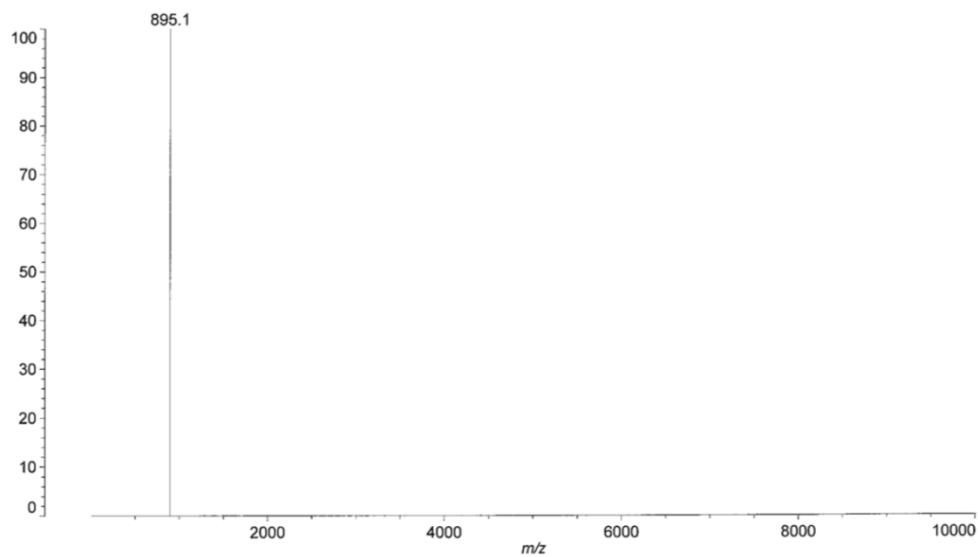
Table of Contents

Information	Page
Mass analysis of CRTpep (Supplemental Figure 1).	S3
Mass analysis of CRTpep-FITC (Supplemental Figure 2).	S4
Mass analysis of ¹⁹F-CRTpep (Supplemental Figure 3).	S5
Cytotoxicity of immunogenic and non-immunogenic drugs against CT26 cells (Supplemental Figure 4).	S6
Evaluation of apoptosis induced in CT26 cells by non-immunogenic and immunogenic drugs (Supplemental Figure 5).	S7
Analysis of translocated CRT by flow cytometry using a CRT-specific primary antibody (Supplemental Figure 6).	S8
Fluorescence microscopic analysis of <i>in vivo</i> expression of ectoCRT in immunogenically treated CT26 tumors (Supplemental Figure 7).	S10
Determination of the binding affinity of CRTpep to the recombinant CRT protein (Supplemental Figure 8).	S11
Flow cytometry analysis of CRTpep binding to ecto-CRT after immunogenic and non-immunogenic drug treatment in B16F10 cells (Supplemental Figure 9).	S12

Immunofluorescence staining and analysis of CRTpep binding to ecto-CRT after immunogenic and non-immunogenic drug treatment in B16F10 cells (Supplemental Figure 10).	S13
<i>In vitro</i> and <i>in vivo</i> Stability of ¹⁸F-CRTpep (Supplemental Figure 11).	S14
<i>In vitro</i> uptake of ¹⁸F-CRTpep in CT26 cells (Supplemental Figure 12).	S15
Therapeutic effect of immunogenic and non-immunogenic drugs (DXR, OXP, GEM), and radiation in CT26-tumor bearing mice (Supplemental Figure 13).	S16
Assessment of ICD by animalPET using ¹⁸F-CRTpep in B16F10 tumor-bearing mice. (Supplementary Figure 14).	S17
Biodistribution of ¹⁸F-CRTpep (Supplemental Table 1).	S18

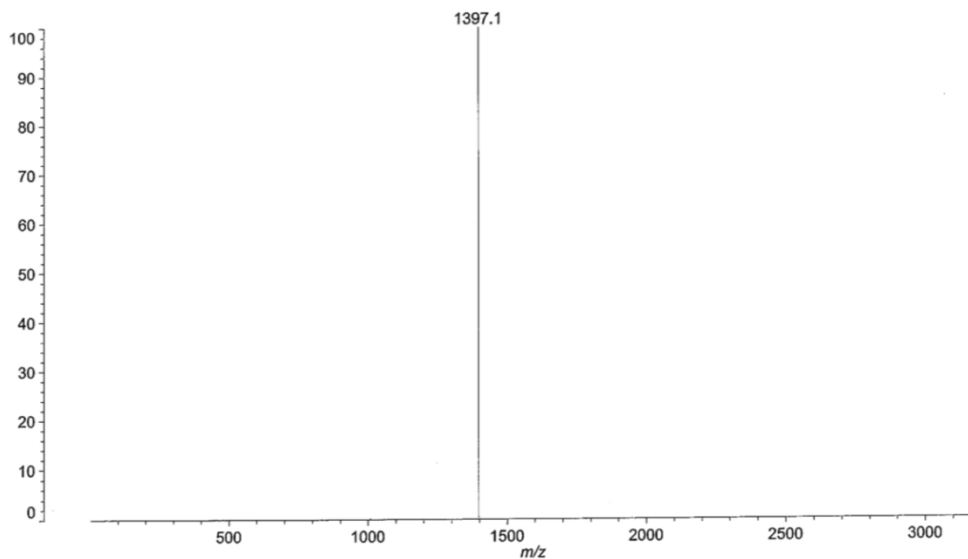
1

ANYGEN
K201734
Data: <Untitled>.C7[c] 5 Aug 2020 9:40 Cal: 7 Apr 2015 20:50
Shimadzu Biotech Axima Assurance 2.9.3.20110624: Mode Linear_20190614, Power: 30, P.Ext. @ 1000 (bin 56)
%Int. 143 mV Profiles 1-200: Threshold 25% Centroid [Adaptive]



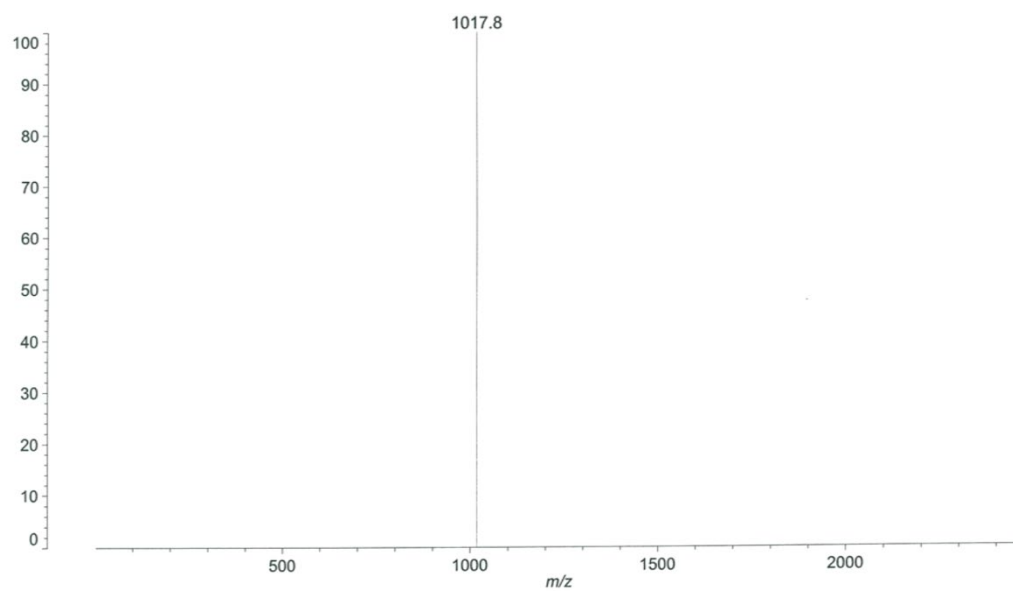
- 1
- 2 **Supplemental Figure 1.** Mass analysis of CRTpep. MS m/z expected $[M]^+ = 895.1$ Da; actual = 891.5 Da.
- 3

AnyGen
K151172
Data: <Untitled>.P23[c] 1 Dec 2015 14:55 Cal: 4000-7000 10.31 31 Oct 2015 14:07
Shimadzu Biotech Axima Assurance 2.9.3.20110624: Mode Linear, Power: 19, P.Ext. @ 5000 (bin 101)
%Int. 3621 mV Profiles 1-5: Threshold 25% Centroid [Adaptive]

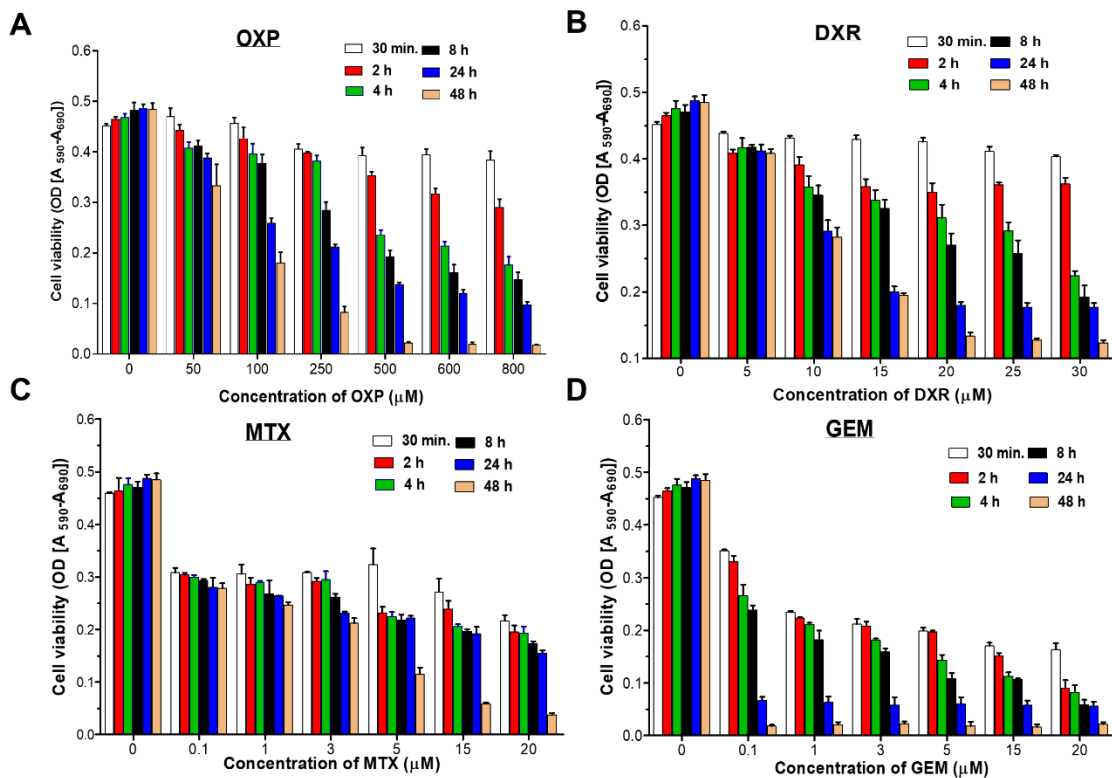


- 1
- 2 **Supplemental Figure 2.** Mass analysis of CRTpep-FITC. MS m/z expected $[M]^+ = 1397.7$ Da; actual =
- 3 1397.1 Da.

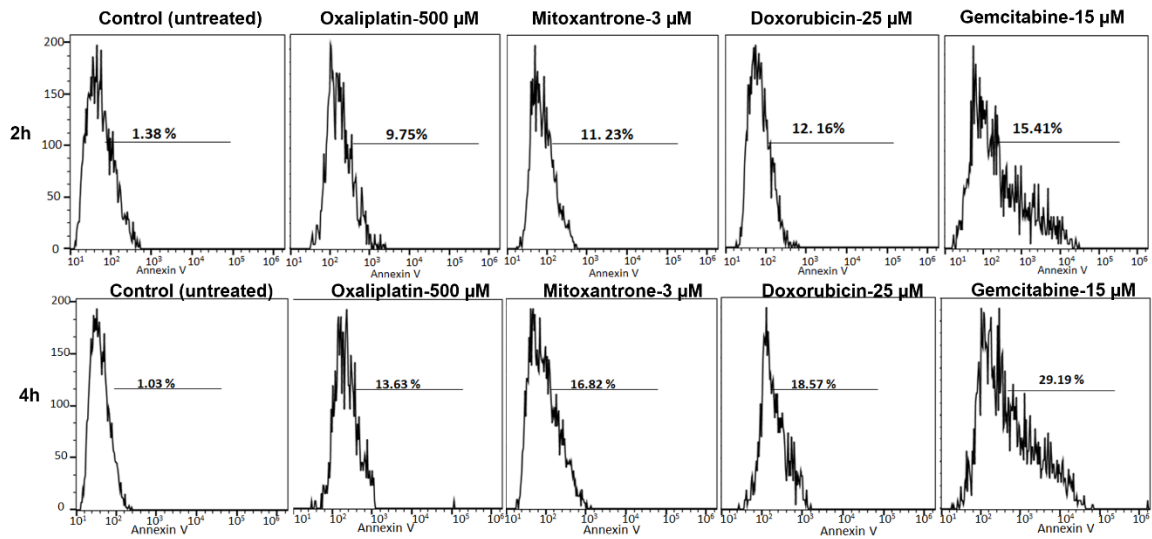
AnyGen
K151171
Data: <Untitled>.J22[c] 1 Dec 2015 14:48 Cal: 4000-7000 10.31 31 Oct 2015 14:07
Shimadzu Biotech Axima Assurance 2.9.3.20110624: Mode Linear, Power: 15, Blanked, P.Ext. @ 4000 (bin 90)
%Int. 547 mV Profiles 1-8: Threshold 25% Centroid [Adaptive]



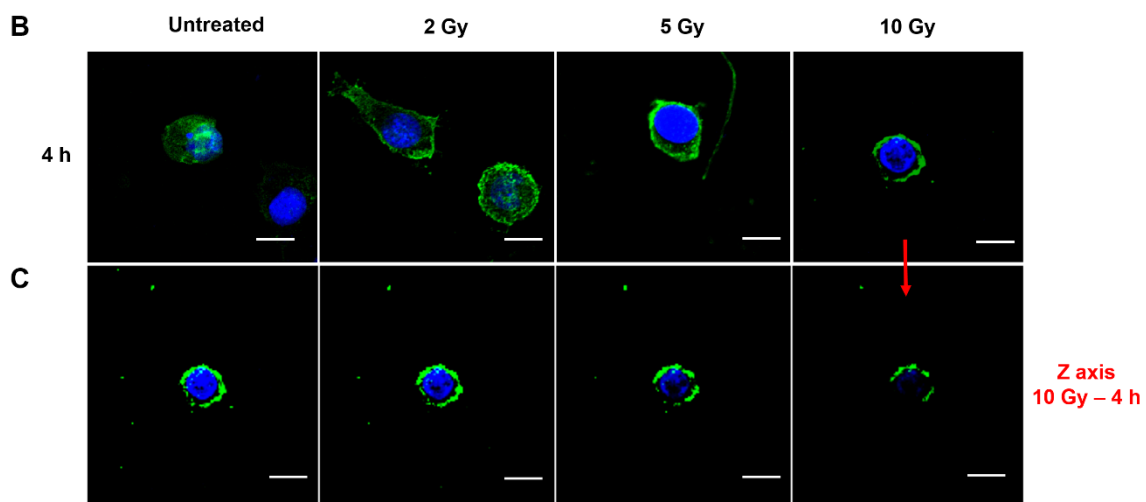
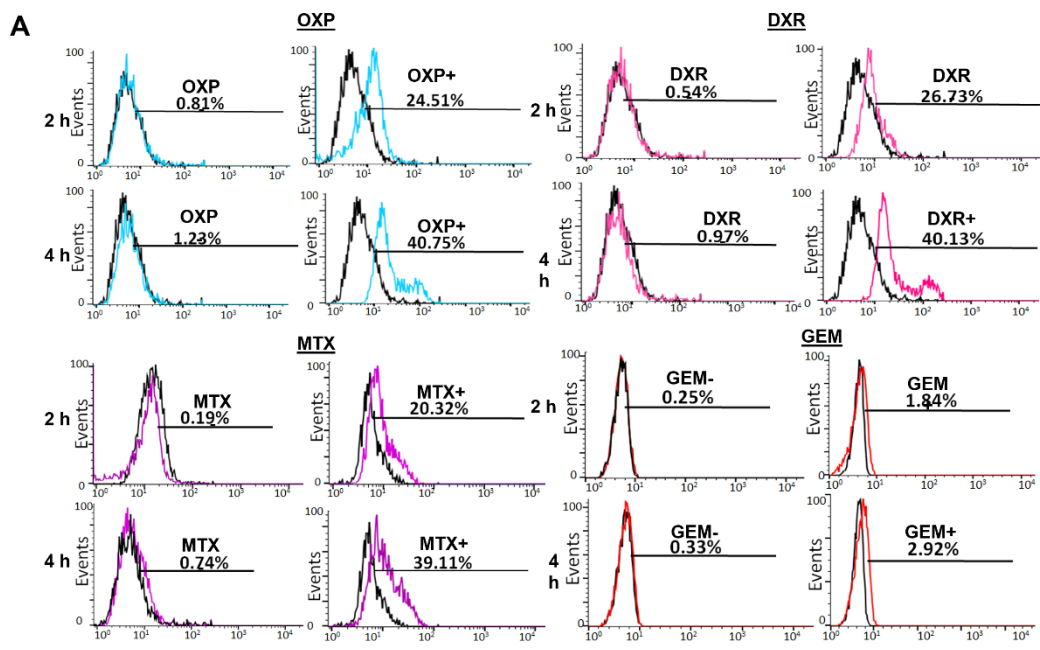
1
2 **Supplemental Figure 3.** Mass analysis of ^{19}F -CRTpep. MS m/z expected $[\text{M}]^+ = 1018.2$ Da; actual =
3 1017.8 Da.
4



1
2 **Supplemental Figure 4.** Cytotoxicity of immunogenic and non-immunogenic drugs against CT26 cells.
3 CT26 cells were cultured with immunogenic drugs (A) oxaliplatin (OXP), (B) doxorubicin (DXR), (C)
4 mitoxantrone (MTX), and (D) the non-immunogenic drug gemcitabine (GEM) for the indicated times.
5 Cell viability was measured using absorbance levels, the level of absorbance was calculated and
6 expressed as the mean ± SD of three independent experiments.



1
2 **Supplemental Figure 5.** Evaluation of apoptosis induced in CT26 cells by non-immunogenic and
3 immunogenic drugs. Apoptotic death was assessed after treatment of CT26 cells with OXP (500 μM),
4 DXR (25 μM), MTX (3 μM), or GEM (15 μM) for 2 and 4 h. Apoptotic induction was assessed using
5 FITC-conjugated annexin-V and flow cytometry. The cell populations binding annexin-V (%) were gated
6 and the percentage of apoptotic cells calculated.



1

2 **Supplemental Figure 6.** (A) Analysis of translocated CRT by flow cytometry using a CRT-specific

3 primary antibody. CT26 cells were treated with or without immunogenic (500 μ M OXP, 25 μ M DXR, 3

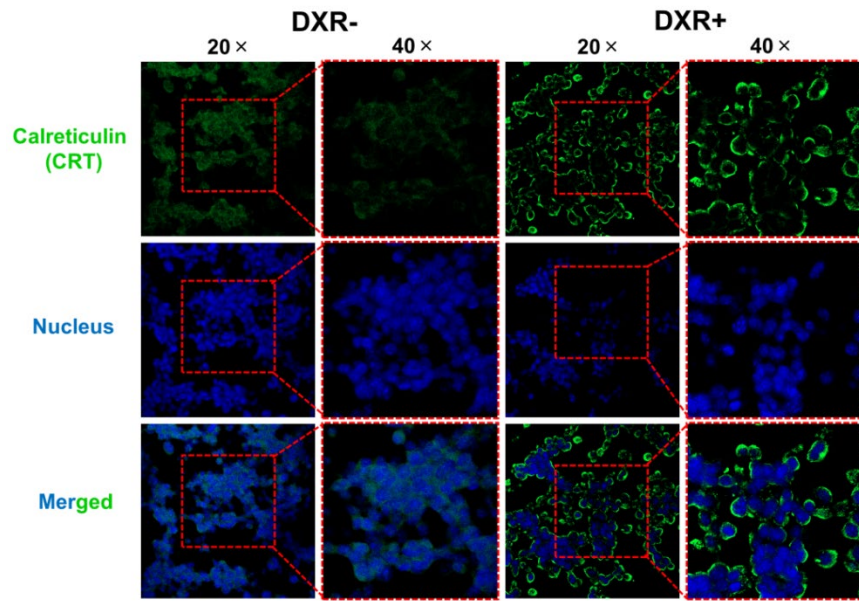
4 μ M MTX) and non-immunogenic (15 μ M GEM) drugs for 2 h or 4 h and then incubated with an anti-

5 CRT antibody followed by an Alexa Fluor 488 secondary antibody to detect the ecto-CRT. The

6 percentage of cells expressing ecto-CRT was calculated based on detected fluorescence levels (compared

1 with the respective control group). (B) Confocal fluorescence microscopy analysis for CRT exposure in
2 irradiated CT26 cells. CT26 cells were irradiated at the indicated doses (2, 5, and 10 Gy) for 4 h and 24 h.
3 The ecto-CRT was detected using an anti-CRT antibody (green) and nuclei were stained with DAPI
4 (blue). Specific binding of CRT-antibody with ecto-CRT in CT26 cells after irradiation was observed
5 using alexa fluor-488 labelled antibody under confocal laser scanning microscopy. Scale bar, 10 μm . (C)
6 Representative confocal Z-slices are shown (arrow). Three-dimensional reconstruction sections are shown
7 with fluorescence (Z section). Scale bar = 10 μm

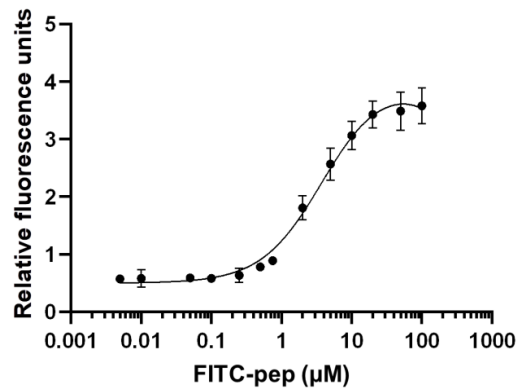
8



1

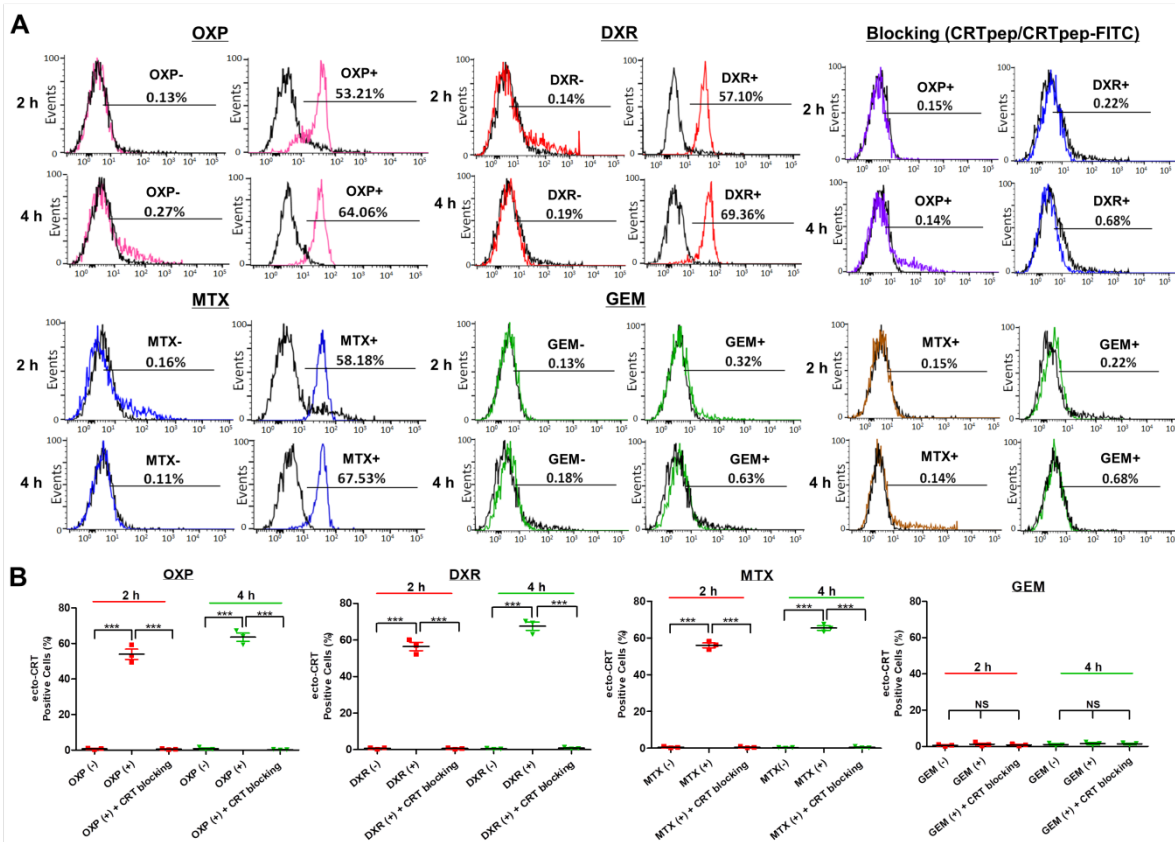
2 **Supplemental Figure 7.** Fluorescence microscopic analysis of *in vivo* expression of ectoCRT in
 3 immunogenically treated CT26 tumors. CT26 cells bearing tumor xenografts were treated with DXR (10
 4 mg/kg) and the ectoCRT expression was detected using CRT specific antibody by confocal laser scanning
 5 microscopy (20 × and 40 × magnification). Image shows the, Green, CRT-antibody with Alexa 488
 6 stained ectoCRT; blue and DAPI-stained nuclei.

7

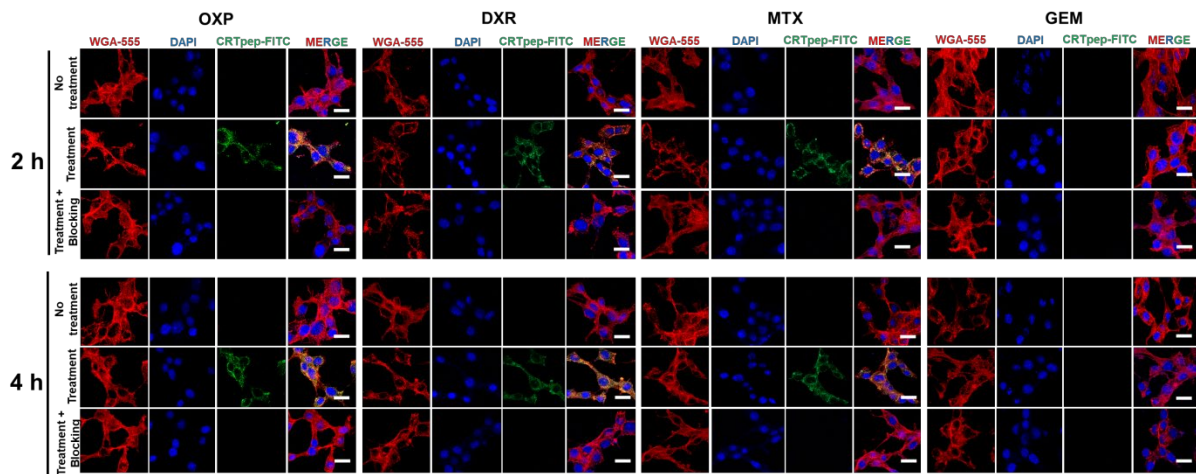


1
2 **Supplemental Figure 8.** Determination of the binding affinity of CRTpep to the recombinant CRT
3 protein. Recombinant CRT (0.1 μg) were captured per well of 96 well ELISA plate and different
4 concentration of FITC-CRTpep (100.0, 75.0, 50.0, 20.0, 10.0, 5.0, 2.0, 1.0, 0.75, 0.50, 0.25, 0.10, 0.05,
5 0.01, 0.005, 0.0 μM) were allowed to bound for 2 h at room temperature. Fluorescence intensity were
6 measured and K_d value were calculated by nonlinear regression (curve fit) GraphPad Prism (K_d value of
7 CRTpep= 1.868 μM).

8

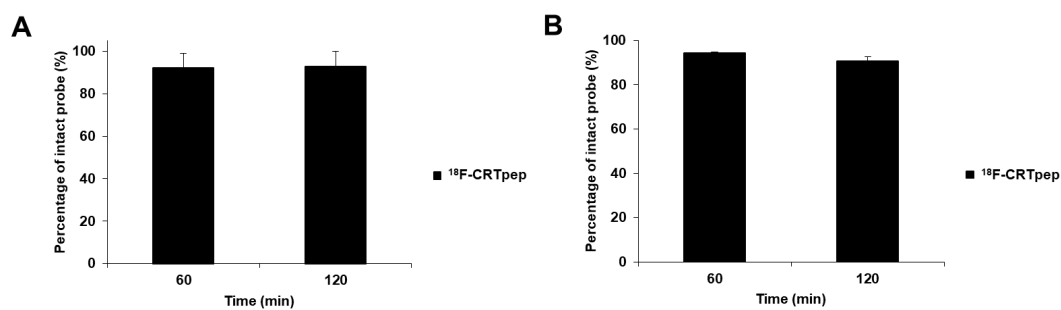


1
2 **Supplemental Figure 9.** Flow cytometry analysis of CRTpep binding to ecto-CRT after immunogenic
3 and non-immunogenic drug treatment in B16F10 cells. (A) Flow cytometry analysis of CRTpep binding
4 to ecto-CRT after immunogenic and non-immunogenic drug treatment in B16F10 cells. Binding of
5 CRTpep-FITC to ecto-CRT in in B16F10 cells after 2 h and 4 h of anticancer drug (immunogenic and
6 non-immunogenic) treatment was determined by flow cytometry. Percentage cellular uptake was
7 calculated based on the detected mean fluorescence levels of untreated control cell. After anticancer drug
8 treatment in B16F10 cells were pre-incubated with CRTpep (200 μ M) for 1 h, followed by incubation
9 with CRTpep-FITC (2 μ M), and then was subjected to flow cytometry to detect uptake using fluorescence
10 generated by the ecto-CRT. (B) Quantitative assessment of binding of CRTpep-FITC to ecto-CRT in in
11 B16F10 cells after 2 h and 4 h of anticancer drug (immunogenic and non-immunogenic) treatment that
12 was determined by flow cytometry. The data were analyzed with one-way ANOVA method and
13 expressed as mean (\pm SD) fluorescence level. (n = 3; *** P < 0.001; ns = not significant).



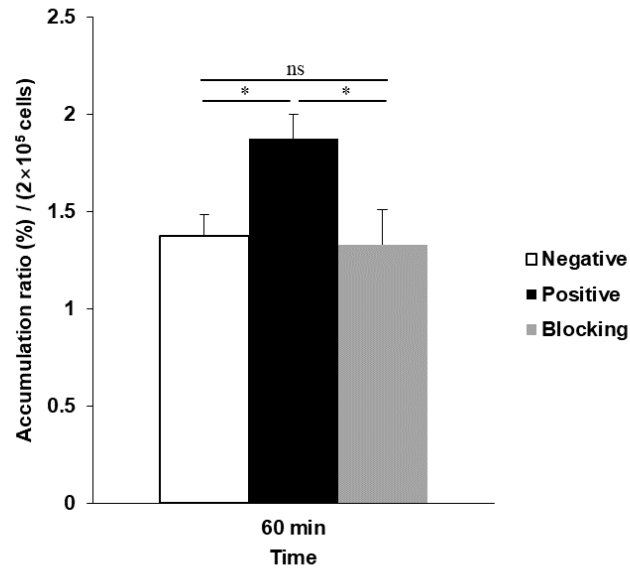
1
 2 **Supplemental Figure 10.** Immunofluorescence staining and analysis of CRTpep binding to ecto-CRT
 3 after immunogenic and non-immunogenic drug treatment in B16F10 cells. Binding of CRTpep-FITC to
 4 ecto-CRT in B16F10 cells after 2 h and 4 h of anticancer drug (immunogenic and non-immunogenic)
 5 treatment was determined by confocal laser scanning microscopy (40 × magnification) after
 6 immunofluorescence staining. Green, CRTpep-FITC; blue, DAPI-stained nuclei; red, cell membrane
 7 stained with WGA-555. Scale bar, 50 μm. For the blocking assay, anticancer drug-treated cells were
 8 further incubated with 200 μM unlabeled CRTpep followed by 2 μM CRTpep-FITC. Scale bar, 50 μm.

9

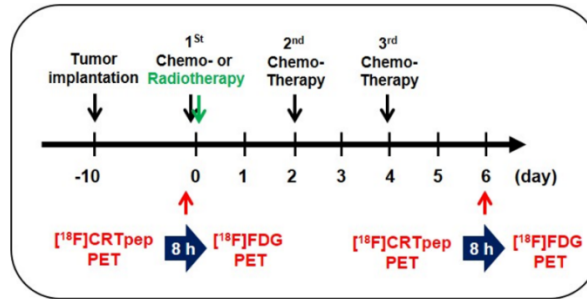
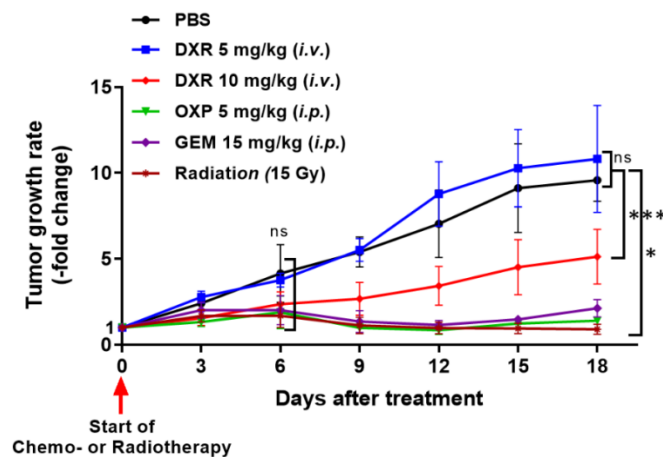


1
2 **Supplemental Figure 11.** Stability of ^{18}F -CRTpep. (A) *In vitro* stability of ^{18}F -CRTpep (0.74 MBq) in
3 human serum at 60 min and 120 min after incubation (92.16 ± 6.80 at 60 min and 92.98 ± 7.16 at 120
4 min). (B) *In vivo* stability of ^{18}F -CRTpep (7.4 MBq/ 100 μL) at 60 min and 120 min incubation ($94.30 \pm$
5 0.63 at 60 min and 90.62 ± 2.12 at 120 min). Stability was then analyzed by instant thin layer
6 chromatography-silica-gel (iTLC-SG) developed with 0.1% TFA in D.W. and 0.1% TFA in acetonitrile
7 (3 : 7) after 60 min and 120 min.

8



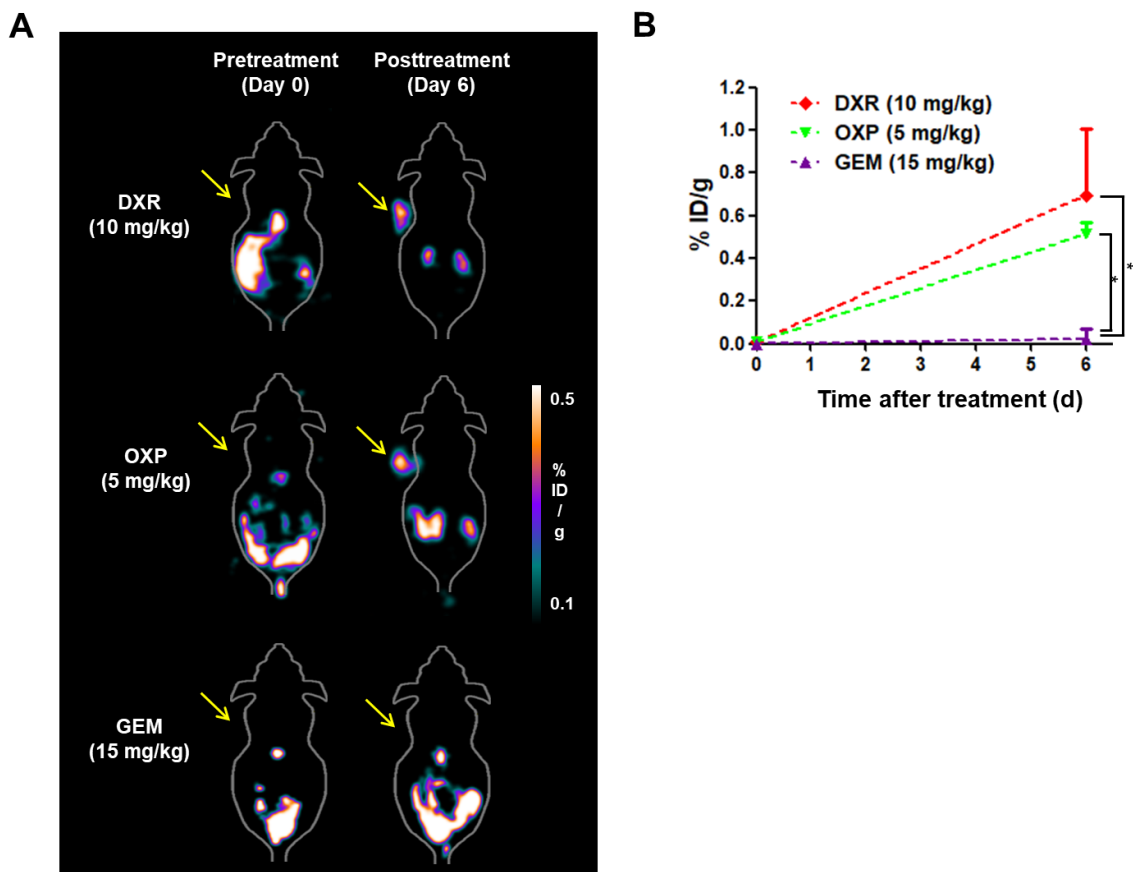
1
2 **Supplemental Figure 12.** *In vitro* cellular uptake of ¹⁸F-CRTpep in CT26 after DXR treatment for 4 h.
3 Blocking group was pretreated with CRT antibody (1 μg/ 0.5 mL) for 1 h. The cells were incubated with
4 0.74 MBq of ¹⁸F-CRTpep for 60 min and washed twice with DPBS. The radioactivity of the supernatant
5 and cell lysate was measured with a gamma counter. Data are expressed as the accumulation ratio (%) ±
6 SD per 2 × 10⁵ cells (Pyo et al. J Nucl Med 2018; 59:340–346). It was calculated by dividing the
7 radioactivity in the pellet by the radioactivity in the supernatant and pellet combined. (Negative, Positive,
8 Blocking group: 1.38 ± 0.11, 1.88 ± 0.12, 1.33 ± 0.18 at 60 min, **P* < 0.05; ns = not significant)

A**B**

1
2 **Supplemental Figure 13.** Therapeutic effect of immunogenic and non-immunogenic drugs (DXR, OXP,
3 GEM), and radiation in CT26-tumor bearing mice. (A) CT26- bearing mice were injected intravenously
4 (*i.v*) or intraperitoneally (*i.p*) with DXR (5 mg/kg or 10 mg/kg), OXP (5 mg/kg), GEM (15 mg/kg), or
5 PBS three times with a 2 day interval between each dose. Radiation (15 Gy) was given once. ¹⁸F-CRTpep
6 and ¹⁸F-FDG animalPET were performed at 8-h intervals in the same animals. (B) Tumor growth rate was
7 measured at indicated days after chemo- and radiation therapy (n = 6; **P* < 0.05; ****P* < 0.001; NS = not
8 significant; *P* value of PBS vs DXR (5 mg/kg), DXR (10 mg/kg), OXP, GEM, or radiotherapy on day 6: >
9 0.9999, = 0.6173, = 0.1416, = 0.195,5 or = 0.0804, respectively; *P* value of PBS vs DXR (5 mg/kg), DXR
10 (10 mg/kg), GEM, or radiotherapy on day 18: > 0.9999, = 0.0006, = 0.0167, or = 0.0025, respectively).

11

12



1
 2 **Supplemental Figure 14.** Assessment of ICD by small animal PET using ^{18}F -CRTpep in B16F10 tumor-
 3 bearing mice. (A) Representative ^{18}F -CRTpep small animal PET images of B16F10-bearing mice. ^{18}F -
 4 CRTpep (7.4 MBq) was injected (*i.v.*) into mice before and at 6 days after chemotherapy. Arrows indicate
 5 subcutaneous tumors. (B) Quantification of ^{18}F -CRTpep small animal PET imaging signals in tumors
 6 before (day 0) and after treatment (DXR = 0.70 ± 0.31; OXP = 0.51 ± 0.06; GEM = 0.02 ± 0.04; * P <
 7 0.05).

8

1 **Supplemental Table 1.** Biodistribution of ^{18}F -CRTpep at 120 min after *i.v.* injection in CT26 tumor
2 bearing mice 6 days after DXR treatment. Tumor, blood, and other organs were extracted and weighed,
3 and the radioactivity in the organs was counted using a gamma counter. To obtain the %ID/g,
4 radioactivity determinations were normalized against the weight of tissue and the amount of radioactivity
5 injected (n = 4).

Organs	%ID/g
Blood	0.61 ± 0.36
Heart	0.20 ± 0.11
Lung	0.36 ± 0.24
Liver	0.35 ± 0.21
Spleen	0.31 ± 0.24
Stomach	0.17 ± 0.14
Intestine	2.22 ± 0.43
Kidney	4.61 ± 1.24
Pancreas	0.28 ± 0.19
Normal muscle	0.31 ± 0.17
Bone	0.31 ± 0.06
Skin	0.45 ± 0.29
Tumor	0.73 ± 0.34